RIMS Kôkyûroku Bessatsu
B52 (2014), 263–282

The Stokes geometry of the quantum Hénon map in the horseshoe regime

Dedicated to Professor Takashi Aoki on the occasion of his 60th birthday

By

Akira SHUDO*

Abstract

The Stokes geometry for the propagator of the quantum Hénon map is studied in the light of recent developments of the exact WKB analysis, especially in the case where the Hénon map satisfies the horseshoe condition. Our analysis reveals that the birth and death of the WKB solutions caused by the Stokes phenomenon do not occur in a local but entirely global manner, reflecting topological nature encoded in the Stokes geometry. We derive an explicit general formula to enumerate the number of WKB solutions in the asymptotic region and obtain its growth rate, which is shown to be less than the topological entropy of the corresponding classical dynamics.

§ 1. The Hénon map and its quantum propagator

The purpose of this report is to discuss the Stokes geometry of the quantum Hénon map in the light of recent developments of the exact WKB analysis. We aim at understanding the global nature of complex orbits associated with *dynamical tunneling*, which takes place in the system with more than one degree of freedom, and can be considered to be a natural extension of energy barrier tunneling.

The system we study is polynomial maps and its quantum counterpart. In particular we will examine the Hénon map closely. The reason for focusing on the Hénon map is as follows. First the Hénon map is the simplest possible polynomial map exhibiting chaos. This fact owes to the classification theorem of Friedland and Milnor [1]. Since the Hénon map is standard in this sense, not only real but also complex dynamics have

Received March 06, 2014. Revised July 31, 2014. Accepted August 03, 2014.
2010 Mathematics Subject Classification(s): 34E20, 37D20.
Key Words: Stokes geometry, saddle point method, Quantum Hénon map, Smale's horseshoe.
*Department of Physics, Tokyo Metropolitan University, Minami-Osawa, Hachioji, Tokyo 192-0397, Japan. e-mail: shudo@tmu.ac.jp

been and are being studied extensively. Second the quantum version of the Hénon and more general polynomial maps are related to canonical integrals in the complex WKB analysis. In particular, the integral given as one-step quantum propagator is essentially equivalent to the Airy function. The latter is known to be one of the most fundamental integrals in the complex WKB analysis. In addition, the quantum propagator for more general polynomial maps can be connected with integrals given as the diffraction catastrophe integrals [2, 3].

§ 1.1. Quantum propagator and the action for symplectic maps

The standard procedure to formulate quantum mechanics of the symplectic map is to give the unitary operator which generates the time evolution of quantum states. This is achieved by introducing a discrete analog of the Feynman-type path integral

$$\langle q_{n+1}|U^n|q_0\rangle = \int_{-\infty}^{\infty}\cdots\int_{-\infty}^{\infty} dq_1 dq_2\cdots dq_n \exp\Big[\frac{1}{\hbar}S(q_0,q_1,\cdots,q_{n+1})\Big]. \tag{1.1}$$

Here we take the coordinate representation. The function $S(q_0,q_1,\cdots,q_{n+1})$ is the discrete action functional, or the action for short, which is expressed as

$$S(q_0,q_1,\cdots,q_{n+1}) = \sum_{j=1}^{n+1}\frac{1}{2}(q_j-q_{j-1})^2 - \sum_{j=1}^{n}V(q_j), \tag{1.2}$$

where $V(q)$ represents the potential function. This form of the action is determined so that imposing the variational condition on $S(q_0,q_1,\cdots,q_{n+1})$

$$\frac{\partial}{\partial q_i}S(q_0,q_1,\cdots,q_{n+1}) = 0, \quad (1\le i\le n)$$

leads to the symplectic map in the Lagrangian form

$$f : (q_{i+1}-q_i)-(q_i-q_{i-1}) = -\frac{dV(q_i)}{dq_i}. \tag{1.3}$$

Hereafter we fix the initial condition as $q_0 = \text{const}$, and regard $\langle q_{n+1}|U^n|q_0\rangle$ only as a function of q_{n+1}, and q_0 as a fixed parameter. Thus we will use the notation $u(q_{n+1})$ instead of $\langle q_{n+1}|U^n|q_0\rangle$.

Putting $p_{i+1} = q_{i+1} - q_i$ the Lagrangian form (1.3) is rewritten as the symplectic map in the Hamiltonian form:

$$F : \begin{pmatrix} p_{i+1} \\ q_{i+1} \end{pmatrix} = \begin{pmatrix} p_i - V'(q_i) \\ q_i + p_{i+1} \end{pmatrix}. \tag{1.4}$$

In the following discussion, we assume that $V(q)$ is a polynomial of q, and the map derived here is called the polynomial map.

§ 1.2. The Hénon map and pruning of the horseshoe

Among various possibilities, the most canonical choice of $V(q)$ within a class of polynomial maps would be

$$V(q) = -\frac{1}{3}q^3 - cq. \tag{1.5}$$

This is justified by the fact that the map F is transformed via the affine change of the variables $(p, q) = (y - x, 1 - x)$ into one of the standard forms of the Hénon map

$$f_a : \begin{pmatrix} x_{i+1} \\ y_{i+1} \end{pmatrix} = \begin{pmatrix} -x_i^2 - y_i + a \\ x_i \end{pmatrix}, \tag{1.6}$$

where $a = -c - 1$. As mentioned, the classification theorem for polynomial diffeomorphisms on $\mathbb{R}^2$ claims that nontrivial maps are expressed as compositions of Hénon maps [1].

The area-preserving Hénon map f_a has one system parameter a, which controls the qualitative nature of dynamics. Although the Hénon map is known as the most canonical 2-dimensional diffeomorphism, the dynamics is far from completely understood as compared to its 1-dimensional counterpart: the quadratic map $g_a(x) = a - x^2$. Among characteristic parameter regions of a, the simplest situation is realized for large $|a|$ regions. It was proved that for sufficiently large but negative $|a|$ the non-wondering set Λ becomes empty whereas for sufficiently positive a values the dynamics of f_a is described by the horseshoe map [4].

As we vary a from the horseshoe parameter locus, at a certain parameter value, which could be evaluated numerically as $a_f = 5.699\ldots$ [5], the first homoclinic bifurcation between the innermost stable and the outermost unstable manifolds occurs. This event is called the *first tangency*. After the first tangency the dynamics becomes immensely complicated. A possible approach to characterize the dynamics after the first tangency has been proposed in [6, 7]. The idea of the *pruning front* is an analog of kneading theory; it intends to provide a border in the two-dimensional symbol plane which determines admissible and non-admissible orbits.

§ 2. Turning points and Stokes curves

§ 2.1. The saddle point method

The semiclassical analysis we are concerned with is to evaluate the integral (1.1) based on the saddle point method, or the method of steepest descents. For single integrals, it might be possible to identify the saddles that are responsible for the saddle

evaluation by actually drawing steepest descent contours. Since there is only a single integration variable for single integrals, steepest descent contours form a one-dimensional curve in $\mathbb{C}$.

For multiple integrals, on the other hand, several issues exist although it looks formally the same as in the case of single integrals. One has to push the integration contour in $\mathbb{C}^n$ toward the directions of steepest descent, forming a chain of integration hypersurfaces. The multi-dimensional version of steepest descent curves has been examined by Pham who showed that an arbitrary integral hypersurface without boundaries can be replaced by a sum of integration cycles, called Lefschetz thimbles, each of which passes through a single saddle point and along which the real part of the phase function decreases with constant imaginary phase, that is, forming a steepest descent hypersurface [11].

The global aspect in the saddle point method concerns how to find the decomposition into steepest descent hypersurfaces, each of which passes through a single saddle point in generic situations, and how to describe the topological change of such steepest descent hypersurface with a change of parameters. As in the single integral case, switching of steepest descent hypersurfaces happens, nothing more than the multi-dimensional version of the Stokes phenomenon, when two saddle points are shared by a single steepest descent hypersurface.

So far, however, no general and analytical or even numerical method to find a proper decomposition into steepest descent hypersurfaces and thus to describe the associated Stokes phenomenon in such multiple integrals have not been known, except for using hyperasymptotic expansions, in which the adjacency structure of saddles could be extracted from the remainder terms of asymptotic expansions [12, 13, 14]. The algorithm has been extended even to the case where integral contours have boundaries [15].

In Ref. [8], together with the determination of coordinate-wise hypersurfaces [16, 17], and the analysis in the asymptotic region, we have employed the proposed method based on hyperasymptotic expansions to the integral (1.1), and found that these independent methods predict the same global characters and are consistent with each other. Moreover, as a more convenient tool, although not verified in a rigorous way, the single-valuedness of the asymptotic solution is an efficient machinery to fix the Stokes coefficients. As described below, we will adopt this strategy to determine the Stokes coefficients in the present case.

§ 2.2. Turning points and Stokes curves

The most important ingredients for the Stokes geometry are turning points and Stokes curves. For the Stokes geometry of single integrals, turning points are introduced as those points in the parameter space at which two of saddle points of the phase function

coalesce. To be concrete, let q_2^T be a turning point of the propagator (1.1) with $n = 1$. For a given q_2^T, we generally obtain two distinct saddle points, which satisfy the saddle point condition

$$\frac{d}{dq_1} S(q_0, q_1, q_2^T) = 0. \tag{2.1}$$

In order to make two saddle points coalesce, we impose the condition

$$\frac{d}{dq_1} q_2(q_1, q_0) = 0. \tag{2.2}$$

The associated Stokes curves are also defined as those curves fulfilling the condition

$$\mathrm{Re}\, S(q_0, q_1^{(1)}, q_2^T) = \mathrm{Re}\, S(q_0, q_1^{(2)}, q_2^T). \tag{2.3}$$

Here $q_1^{(1)}$ and $q_1^{(2)}$ denote the solutions of the saddle point condition (2.1), and $S(q_0, q_1^{(i)}, q_2^T)$ $(i = 1, 2)$ corresponding actions.

In the conventional argument on Stokes phenomena turning points and Stokes curves are introduced in the same way, and these have been considered to be all ingredients describing the Stokes phenomena. However, Berk, Nevins and Roberts have pointed out, in their analysis of a certain 3rd order ordinary differential equation and its solution in the integral representation, that one has to take into account additional objects what they called *new Stokes curves*, in order to make WKB solutions single-valued [9]. Ad-hoc arguments developed in [9] have later been formulated within the exact WKB framework, combined with the micro-local analysis [10], and further discussed [18, 19].

A crucial difference between 2nd and higher order cases is that all the Stokes curves emanate from the *ordinary turning points* in 2nd order differential equations, whereas there appear new Stokes curves which are not associated with ordinary turning points. These new ingredients, new Stokes curves and associated turning points, now called *virtual turning points*, have been proposed to contribute to the Stokes geometry for higher order differential equations [10].

For our multiple integrals (1.1), since we obtain more than two saddle points in general, we may expect that new components thus introduced come into play as well. In order to introduce the Stokes geometry of our integrals, we should note that the components of the Stokes geometry have been defined only for differential equations so far, especially relying on general theory on the propagation of singularities in differential equations [20]. The propagation of singularities for partial differential equations, which are given as the Borel transform of the original ordinary differential equations, is controlled by the bicharacteristic strip [10, 20, 18, 19].

For our integrals (1.1), we could indeed obtain differential operators acting on our integral [8], and through the recipe thus developed we have defined all the ingredients for

constructing the Stokes geometry. On the basis of such an argument, we say the point q_{n+1}^T is a turning point in the ordinary sense if the following conditions are satisfied

$$\frac{d}{dq_1} q_{n+1}^T(q_0, q_1) = 0, \tag{2.4}$$

$$\frac{d}{dq_1} S\big(q_0, q_1, \cdots, q_{n+1}^T(q_0, q_1)\big) = 0. \tag{2.5}$$

On the other hand, we define the virtual turning point q_{n+1}^T through the conditions

$$q_{n+1}^T(q_0, q_1^{(i)}) = q_{n+1}^T(q_0, q_1^{(j)}) \tag{2.6}$$

$$S(q_0, q_1^{(i)}, \cdots, q_{n+1}^T(q_0, q_1^{(i)})) = S(q_0, q_1^{(j)}, \cdots, q_{n+1}^T(q_0, q_1^{(j)})), \tag{2.7}$$

for $q_1^{(i)} \neq q_1^{(j)}$. In addition, Stokes curves are defined as those curves emanating from the turning point and satisfying

$$\mathrm{Re}\, S(q_0, q_1^{(i)}, \cdots, q_n^{(i)}, q_{n+1}^T) = \mathrm{Re}\, S(q_0, q_1^{(j)}, \cdots, q_n^{(j)}, q_{n+1}^T). \tag{2.8}$$

Note that these definitions are just an extension of turning points and Stokes curves for single integral cases (2.1)-(2.3). Stokes curves emanating from virtual turning points are sometimes called *new Stokes curves*, but what was validated in [10, 18, 19] is that there are essentially no distinctions between new Stokes curves and ordinary ones.

§ 3. Stokes geometry for the horseshoe map

In this section, we analyze the Stokes geometry for the quantum Hénon map in the horseshoe regime. In particular, we will derive an explicit formula for the number of contributing tunneling branches for an arbitrary time step n.

§ 3.1. Generation of ordinary turning points and Stokes curves

We first demonstrate a typical Stokes geometry in the horseshoe regime. The Stokes geometry is composed of ordinary and new Stokes curves, each of which emanates from the corresponding ordinary and virtual turning points respectively. We first show in Fig.1 only the ordinary Stokes curves . As is seen, the ordinary Stokes curves emanating from the same ordinary turning point cross with each other at some points on the real axis, and rotate around the origin.

As explained, the underlying classical time evolution is given as the repetition of stretching and folding and new folding points appear at each time step, doubling their number. Since the ordinary turning points of the Stokes geometry correspond to the folding points of the classical manifold, a sequence of ordinary turning points on the real axis follows exactly that created in classical dynamics. Therefore they appear under a

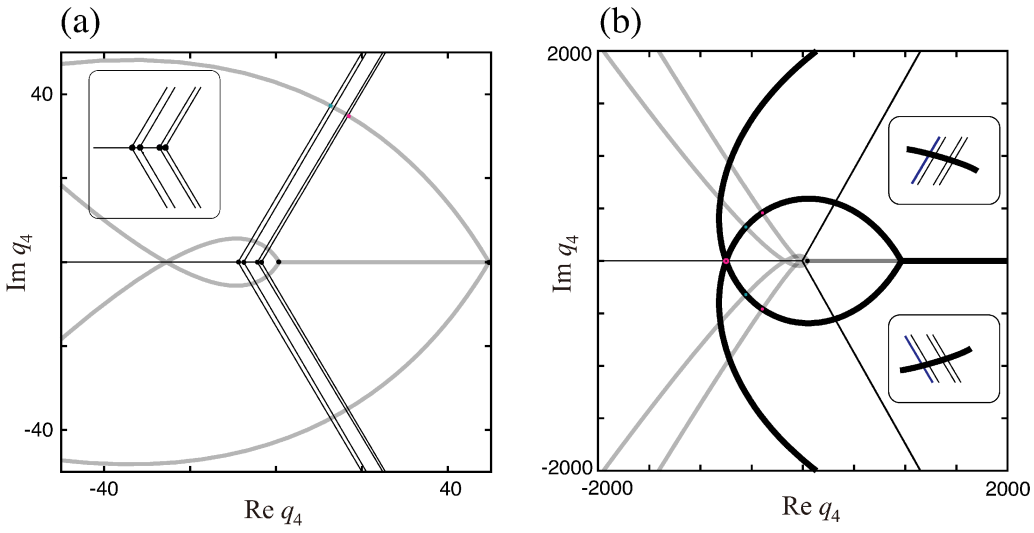

Figure 1. The ordinary Stokes curves for $n = 3$ with the values of parameters $c = -6.0$ and $q_0 = 0$. The bold, gray and thin curves are Stokes curves for the 1st, 2nd and 3rd generation, respectively(see text). The inset in (a) shows the magnification around the ordinary turning points for the 3rd generation and that in (b) indicates the crossing points between the Stokes curves for the 1st and 3rd generation outside the range of this scale.

certain fixed rule in each time step. We show the ordinary Stokes curves schematically in Fig.2, in which the corresponding classical manifolds are also presented for comparison.

The folding point of the one-step manifold corresponds to the turning point for the one-step propagator ($n = 1$) and three Stokes curves emanate from it, as shown in the leftmost column of Fig.2(a). In case of $n = 2$, newly created folding points emerge and the old folding point is switched to move rightward. The corresponding Stokes graph is shown Fig.2(b). In the same way, there are four newly created folding points, and the corresponding turning points in the Stokes geometry for $n = 3$. The ordinary turning points and associated ordinary Stokes curves appear in such a systematic manner, we may assign the *generation* to each ordinary turning points and Stokes curves. That is, the first generated turning points and Stokes curves are called "1st generation", the next generated ones "2nd generation", and "3rd generation", and so on.

In addition to the hierarchy induced in such a way we should note that the position of turning points on the real axis also reflects the nature of the horseshoe dynamics: As schematically illustrated in Fig.2, and could be confirmed in actual numerical calculations, the ordinary turning points lie in the order of the generation on the real axis. We see in Fig.1 that this is indeed the case for $n = 3$. The turning point for the 1st generation takes the rightmost position and those for the 2nd generation follow next. This is because the position of folding points diverges to infinity very quickly (more precisely, super-exponentially) once they fall into filtration regions [21]. As a result of the ordering

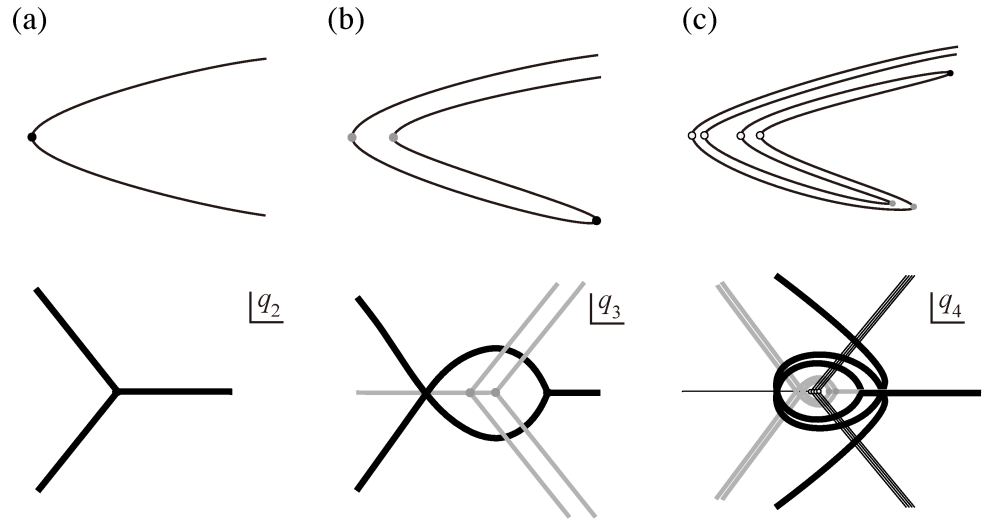

Figure 2. The classical Lagrangian manifolds (upper) and the corresponding ordinary Stokes curves (lower) for (a) $n = 1$, (b) $n = 2$, and (c) $n = 3$. All these are schematic ones. The difference of types of lines distinguishes the generation.

and the rapid separation between turning points belonging to different generations, the crossing points of ordinary Stokes curves at the real axis are also arranged according to the generation: all the crossing points of Stokes curves for the 1st generation (bold curves) appear to the left of all the crossing points for the 2nd generation (gray curves), and so on. In the following, we will assume such an ordering concerning the position of turning points and crossing points of ordinary Stokes curves on the real axis.

§ 3.2. The number of Stokes curves in the q_1-plane

In this subsection we will derive a general formula for the number of crossing points of ordinary Stokes curves on the real axis, which we have observed in the previous subsection. To this end it is useful to consider the Stokes curves on q_1-plane, not on q_{n+1}-plane. Recall that the variable q_1 plays the role of 'time' in the bicharacteristic equations [8].

Let us first consider the $n = 1$ case. In the asymptotic region $|q_2| \to \infty$ one may assume $|q_1|^2 \gg |q_1|$ and $|q_1| \gg |q_0|, |c|$, thus as the leading order the saddle point equation is reduced to $q_1^2 \sim q_2$. This leads to the following two saddle point solutions

$$q_1^{(1)} \sim r^{\frac{1}{2}} e^{\frac{1}{2}i\theta}, \quad q_1^{(2)} \sim -r^{\frac{1}{2}} e^{\frac{1}{2}i\theta},$$

where we put $q_2 = re^{i\theta}$. For $r \to \infty$, the action for each saddle point behaves as

$$S^{(1)} \sim -\frac{2}{3} r^{\frac{3}{2}} e^{\frac{3}{2}i\theta}, \quad S^{(2)} \sim +\frac{2}{3} r^{\frac{3}{2}} e^{\frac{3}{2}i\theta}.$$

Recall the definition of the Stokes line (2.8), which is equivalent to the condition $\mathrm{Re}\, e^{\frac{3}{2}i\theta} = 0$, and this fixes the directions of Stokes curves in the q_1-plane asymptotically as

$$\frac{1}{2}\theta = \frac{2m_1 - 1}{6}\pi \quad (1 \leq m_1 \leq 6).$$

The same argument can be applied to the case $n = 2$. For $|q_3| \to \infty$, we may assume $|q_1|^2 \gg |q_1|$, $|q_2|^2 \gg |q_2|$, $|q_1|^2 \gg |q_0|, c$ and $|q_2|^2 \gg c$, therefore the saddle point equations are reduced as the leading order to

$$q_1^2 - q_2 \sim 0, \tag{3.1}$$

$$q_2^2 - (q_1 + q_3) \sim 0, \tag{3.2}$$

then we have $q_1^4 \sim q_3$. This leads to four saddle point solutions

$$q_1^{(1)} \sim r^{\frac{1}{4}} e^{\frac{1}{4}i\theta}, \quad q_1^{(2)} \sim ir^{\frac{1}{4}} e^{\frac{1}{4}i\theta}, \quad q_1^{(3)} \sim -r^{\frac{1}{4}} e^{\frac{1}{4}i\theta}, \quad q_1^{(4)} \sim -ir^{\frac{1}{4}} e^{\frac{1}{4}i\theta},$$

and

$$q_2^{(1,3)} \sim r^{\frac{1}{2}} e^{\frac{1}{2}i\theta}, \quad q_2^{(2,4)} \sim -r^{\frac{1}{2}} e^{\frac{1}{2}i\theta}, \tag{3.3}$$

where we put $q_3 = re^{i\theta}$. Since the terms of the action is $q_2^3/3 - q_2 q_3$, for $r \to \infty$ we have

$$S^{(1,3)} \sim r^{\frac{3}{2}} e^{\frac{3}{2}i\theta}, \quad S^{(2,4)} \sim -r^{\frac{3}{2}} e^{\frac{3}{2}i\theta}.$$

In the same way as above, the definition of the Stokes curves , $\mathrm{Re}\, S^{(k)} = \mathrm{Re}\, S^{(\ell)}$ $(k \neq \ell)$, is rewritten as $\mathrm{Re}\, e^{\frac{3}{2}i\theta} = 0$. But the actions for the saddles 1 and 3, and those for the saddles 2 and 4 are degenerated, thus this only provides the directions of Stokes curves in the q_1-plane as

$$\frac{1}{4}\theta = \frac{2m_2 - 1}{12}\pi \quad (1 \leq m_2 \leq 12). \tag{3.4}$$

Note that new Stokes curves appear in the case of $n = 2$, so Stokes curves now in question are not necessarily the ordinary ones, but we cannot distinguish which ones are ordinary Stokes curves and which are not.

In order to resolve degeneracies between 1 and 3, and between 2 and 4, we consider the next leading terms in the action. Due to eq.(3.3), the next leading terms turn out to be $q_1^3/3 - q_2 q_1$. This is exactly the leading order terms in the action for $n = 1$. Hence we obtain the associated directions of Stokes curves as

$$\frac{1}{2}\theta = \frac{2m_1 - 1}{6}\pi \quad (1 \leq m_1 \leq 6). \tag{3.5}$$

The combination of (3.4) and (3.5) provides the directions of Stokes curves in the asymptotic region for the $n = 2$ case.

The same argument can be developed for arbitrary time steps, and the induction will apply to derive a general rule. To this end we assume that the directions of Stokes curves for the n-step case are given as

$$\frac{1}{2^i}\theta = \frac{2m_i - 1}{3 \cdot 2^i}\pi \quad (1 \leq i \leq n,\ 1 \leq m_i \leq 3 \cdot 2^i), \tag{3.6}$$

where we put $q_{n+1} = re^{i\theta}$. The form of the $(n+1)$-step action is rewritten as

$$\begin{aligned} S(q_0, q_1, \cdots, q_{n+2}) &= \sum_{j=0}^{n+2} \frac{1}{2}(q_j - q_{j-1})^2 + \sum_{j=1}^{n+1} \Big(\frac{1}{3}q_j^3 + cq_j\Big) \\ &= S(q_0, q_1, \cdots, q_{n+1}) + \frac{1}{2}(q_{n+2} - q_{n+1})^2 + \frac{1}{3}q_{n+1}^3 + cq_{n+1}. \end{aligned}$$

Putting $q_{n+2} = r'e^{i\theta'}$, the 2^{n+1} saddle points for $r' \to \infty$ are expressed as

$$q_1^{(k)} \sim r'^{\frac{1}{2^{n+1}}} e^{\frac{1}{2^{n+1}} i(\theta' + 2\pi k)} \qquad (0 \leq k \leq 2^{n+1} - 1),$$

and correspondingly, we have

$$q_{n+2}^{2(\ell-1)} \sim r'^{\frac{1}{2}} e^{\frac{1}{2}i\theta'}, \quad q_{n+2}^{2\ell-1} \sim -r'^{\frac{1}{2}} e^{\frac{1}{2}i\theta'} \qquad (1 \leq \ell \leq 2^n).$$

Since the leading order terms in $S(q_0, q_1, \cdots, q_{n+2})$ are $q_{n+1}^3/3 - q_{n+1}q_{n+2}$, we have the action for each saddle point as

$$S^{2(\ell-1)} \sim r'^{\frac{3}{2}} e^{\frac{3}{2}i\theta'}, \quad S^{2\ell-1} \sim -r'^{\frac{3}{2}} e^{\frac{3}{2}i\theta'} \qquad (1 \leq \ell \leq 2^n).$$

Hence Stokes curves in the q_1-plane have directions with the angles

$$\frac{1}{2^{n+1}}\theta' = \frac{2m^{n+1} - 1}{3 \cdot 2^{n+1}}\pi \quad (1 \leq m^{n+1} \leq 3 \cdot 2^{n+1}). \tag{3.7}$$

For pairs of saddle points whose actions are degenerated within the leading order estimations, it is suffice to examine the next leading terms, that is $S(q_0, q_1, \cdots, q_{n+1})$. Because of the assumption of the induction, it turns out that the directions of Stokes curves for $S(q_0, q_1, \cdots, q_{n+1})$ are given as (3.6). This completes the proof.

§ 3.3. The number of intersections of ordinary Stokes curves with the real axis

As schematically shown in Fig.2, ordinary Stokes curves intersect with the real axis, and the number of intersection increases with the number of iteration. Here we will derive a formula for the intersection number at an arbitrary time step.

First we note that one of three ordinary Stokes curves emanating from each ordinary turning point is running along the real axis in the q_{n+1}-plane. We show in Fig.3 the

Stokes geometry for the q_{n+1}-plane and the corresponding Stokes curves drawn in the q_1-plane in the case of $n = 3$. In this case, Stokes curves for the 1st generation that run in the complex q_{n+1}-plane intersect the real axis twice, and intersection points in the q_{n+1}-plane appear in the q_1-plane as points at which ordinary Stokes curves for the 1st generation intersect with Stokes curves of higher generations which run along the real q_{n+1}-axis.

Let N_n be the number of intersection points of ordinary Stokes curves in the first generation on the real q_{n+1}-axis. The above observation implies that we may examine the intersection points in the q_1-plane, instead of examining the behavior in the q_{n+1}-plane

Recall that asymptotic directions of the Stokes curves for the 1st generation are, as discussed above, fixed and do not depend on the time step. Thus, without loss of generality, we may take the Stokes curve whose asymptotic direction is $\pi/6$ (see Fig.3). Furthermore, using the result in the previous subsection it is easy to show that the asymptotic directions of Stokes curves with higher generations which run along the real q_{n+1}-axis are $(k/2^n)\pi$ where $1 \leq k \leq 2^{n-1} - 1$.

If the angle of asymptotic direction of the 1st generation is smaller than that of higher-order generations, the Stokes curves for the 1st generation intersect with those of higher-order generations. Therefore it is sufficient to count the number of k satisfying $\pi/6 < (k/2^n)\pi$, that is

$$2^n < 6k \tag{3.8}$$

in the range of $1 \leq k \leq 2^{n-1} - 1$. This consideration gives the formula

$$N_n = (2^{n-1} - 1) - \Big[\frac{2^{n-1}}{3}\Big]. \tag{3.9}$$

for $n \geq 2$. Here $[x]$ denotes the greatest integer that is less than or equal to x. We list first several concrete values of N_n:

$$N_1 = 0, \quad N_2 = 1, \quad N_3 = 2, \quad N_4 = 5, \quad N_5 = 10, \quad N_6 = 21, \cdots .$$

We further note

$$N_n^{\mathrm{neg}} = \begin{cases} N_n/2 & (n : \text{even}) \\ N_n/2 + 1 & (n : \text{odd}) \end{cases} \tag{3.10}$$

and

$$N_n^{\mathrm{pos}} = N_n - N_n^{\mathrm{neg}},$$

where N_n^{neg} and N_n^{pos} denote the intersection numbers in the negative and positive real q_{n+1}-axis, respectively.

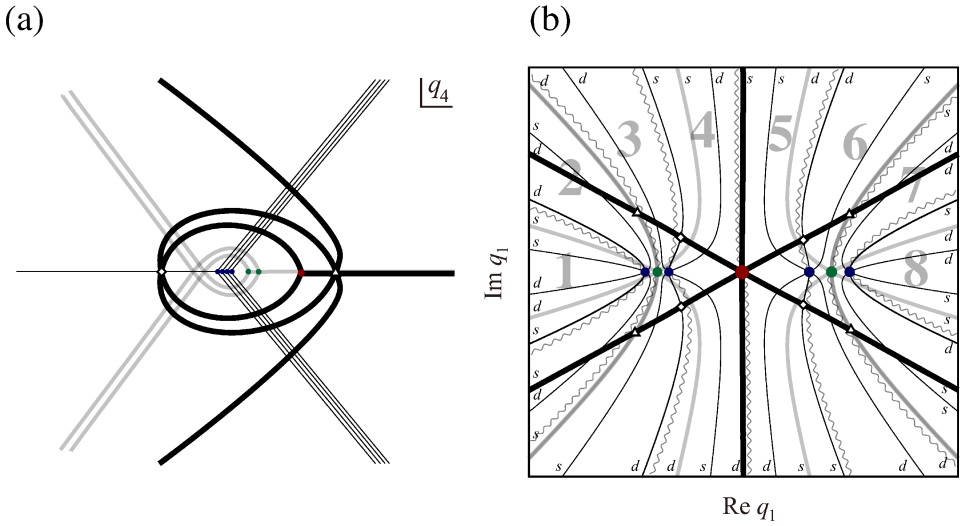

Figure 3. The ordinary Stokes curves for the $n = 3$ case (a) in the q_{n+1}-plane (schematic), and (b) in the q_1-plane. The difference of types of lines distinguishes the generation. The Stokes curves for the lowest generation (bold) intersect with the real q_{n+1}-axis twice. In (b), the cuts are drawn as wavy curves and bold numbers in each sector partitioned by the cuts are the numbers specifying the solution. The dominance relation for each Stokes curve is also attached as 's' or 'd' in (b).

§ 4. Connection along the real axis the growth rate of tunneling solutions

§ 4.1. Multiple crossing points on the real axis and the diagram

In the previous subsections, we have focused solely on the ordinary turning points and associated Stokes curves, but as shown in Fig.4 intersections between ordinary Stokes curves frequently occur. This implies that virtual turning points and new Stokes curves may come into play as well. This is true in general, and indeed multiple crossings appear on the real axis. As presented in Fig.4, the new Stokes curves involved in multiple crossings point are active (solid lines) and the connection occurs on them.

However, as actually shown in the next subsection, as far as the connection along the real axis is concerned, it is not necessary to take into account new Stokes curves. Since we are interested in the propagator connecting q_0 and q_{n+1} and they are observables in quantum mechanics, both should be real. Thus we may only consider the connection along the real axis here. This greatly simplifies our argument.

In order to prove this and for later convenience, we here introduce a diagram which represents the multiple crossing points on the real axis of the q_{n+1}-plane. The diagram consists of three segments (see an example in Fig.4): here the middle segment (bold) represents two Stokes curves, both intersecting with the real axis transversally, and the

other two segments (solid) Stokes curves running along the real axis. The corresponding Stokes curves are depicted in the right row. We here present one example out of 4 possible combinations with respect to the dominance relation for each Stokes curve in Fig.4. Here u_i represents saddle point solutions labelled by the number i. The assignment of the number is given by introducing the cut (wavy curves in the figure) emanating from ordinary turning point. The direction of each cut is chosen in such a way that it is in the same direction as but slightly below the Stokes curve running along the real axis of q_{n+1}- plane (see in the right row of Fig.4). The cuts in the the q_1-plane are drawn also in Fig.3 (b). We can recognize that the cuts drawn in the q_1-plane (see Fig.3 (b)) divide the q_1-plane into the 2^n sectors, to each of which the solution number is assigned.

Using this diagram, multiple crossing points on the real axis in the q_{n+1}-plane, schematically presented in Fig.2, can be represented graphically as shown in Fig.5 for example. We here give the diagrams for the $\mathrm{Re}\, q_{n+1} < 0$ side (left) and the $\mathrm{Re}\, q_{n+1} > 0$ side (right) separately. Each arrow in the figure indicates which solutions are involved the crossing, and the dominance relation, the assignment of 'd' and 's' to each segment, is also automatically determined (see Fig.3).

Obviously, the diagram has a hierarchical structure reflecting the underling horseshoe dynamics: the diagram with a fixed time step is composed of diagrams for the former step. Such a structure will be fully used to analyze the connection rule in the next subsections.

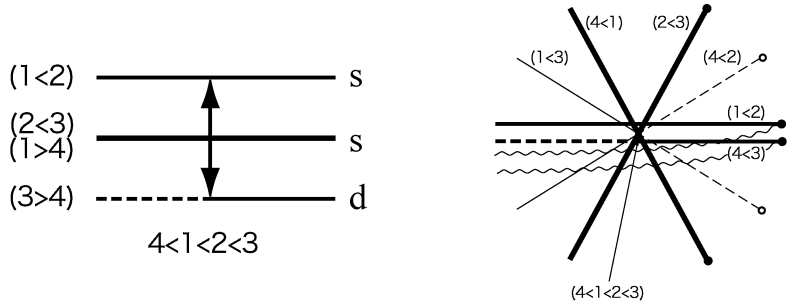

Figure 4. A Possible pattern of multiple crossings on the real axis of the q_{n+1}-plane (rigtht) and the corresponding reduced diagrams (left). The dominance relation on each Stokes curve is denoted by $(i < j)$, meaning that the solution u_j is dominant to u_i. The symbols 's' and 'd' attached in the diagram represent the dominance relation for the associated Stokes line. The symbol 's' means that the numbers i and j appear in the ascending order in the dominance relation $(i < j)$, and vice versa. The middle line (bold) stands for two Stokes curves which intersect the real axis transversally, and the attached symbols 's' and 'd' represent the dominance relation for the upper pair. The thin lines in the right figure show new Stokes curves.

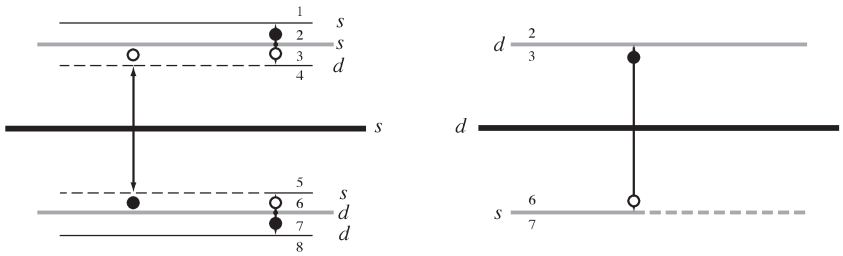

Figure 5. The diagram representing the multiple crossing on the real axis for the $n = 3$ case. The diagram for $\mathrm{Re}\, q_{n+1} < 0$ (left) and for $\mathrm{Re}\, q_{n+1} > 0$ (right).

§ 4.2. The role of new Stokes curves

We now explain why it is not necessary to take into account the connection on the new Stokes curves as far as the connection along the real axis is concerned. For simplicity we consider the connection along and just above the real axis, and in the $\mathrm{Re}\, q_{n+1} < 0$ side. The same argument holds for $\mathrm{Re}\, q_{n+1} > 0$ side as well.

From the diagrams presented in Fig.4, we notice that the most dominant or the second dominant solutions must remain in order to have the connection on the new Stokes curves at each multiple crossing point. For example, in the case presented in Fig.4, the solution u_3 should be retained at the crossing point, otherwise the connection does not occur. In this diagram, the solution u_3 is the most dominant whereas there is another pattern in which u_3 the second dominant. There can appear another patterns in which the solution u_4 should exist.

On the other hand we also know that the most dominant and the second dominant solutions are growing solutions in the real negative direction, *i.e.,* $\mathrm{Re}\, q_{n+1} \to -\infty$, since they are both dominant on the Stokes curves along the real axis.

Now we focus on the leftmost crossing point on the real axis. In Fig.5, the open and filled circles respectively stand for the most dominant and the second dominant solutions in each crossing point. Due to the boundary condition for $\mathrm{Re}\, q_{n+1} \to -\infty$, and there exist no further connections on the left side of the crossing point in question the growing solution in the negative $\mathrm{Re}\, q_{n+1}$ direction should be thrown away, hence the most dominant solution does not remain at this leftmost crossing point. This implies that there exists no solution which kill the second most dominant solution as a result of the connection. However, as noted above, the second dominant solution also explodes as $\mathrm{Re}\, q_{n+1} \to -\infty$, thus we may not keep the second dominant solution as well. Consequently, the most dominant and the second dominant solutions are not allowed to exist at the leftmost crossing point.

We can apply the same argument to the second leftmost crossing point. We may not keep the most dominant one due to the the boundary condition, and for the same reason

above the second dominant solution at this crossing point cannot exist. Repeating this logic, it turns out that the most dominant and the second dominant solutions for all possible crossing points are not allowed to exist. As mentioned, it is necessary to keep the most dominant or the second dominant solutions in order that the connection on the new Stokes curves happens, which leads us to our desired conclusion.

§ 4.3. The connection procedure for arbitrary steps and the number of tunneling branches

We are now free from the complication which might be invoked by new objects, virtual turning points and new Stokes curves, and as a result the connection rules along the real axis become simpler. As explained, ordinary turning points in the Stokes geometry are nothing more than the folding points of the iterated manifold in classical dynamics. Folding points are formed in a well controlled manner as far as the horseshoe condition is satisfied, thus the generation of Stokes curves could be naturally introduced. Here we will show how a simple rule reflecting the underlying horseshoe dynamics is shared by the connection rule along the real axis, which turns out to provide a general formula specifying the contributing of tunneling branches.

We here consider the general connection procedure for an arbitrary step n and finally provide an asymptotic formula for the number of tunneling branches. In what follows, we first define intermediate reference points on the real axis explicitly, which will be convenient to organize the connection rule:

$$
\begin{aligned}
&+(n-1) : \text{right side of } \mathcal{C}_1^R \\
&\quad\cdots \qquad\qquad\quad \cdots \\
&+m \quad\;\; : \text{between } \mathcal{T}_{n-m} \text{ and } \mathcal{C}_{n-m-1}^R \\
&\quad\cdots \qquad\qquad\quad \cdots \\
&+1 \quad\;\; : \text{between } \mathcal{T}_{n-1} \text{ and } \mathcal{T}_{n-2} \\
&O \quad\;\; : \text{between } \mathcal{T}_{n} \text{ and } \mathcal{T}_{n-1} \\
&-1 \quad\;\; : \text{between } \mathcal{C}_{n-1}^L \text{ and } \mathcal{C}_{n-2}^L \\
&\quad\cdots \qquad\qquad\quad \cdots \\
&-m \quad\;\; : \text{between } \mathcal{C}_{n-m}^L \text{ and } \mathcal{C}_{n-m-1}^L \\
&\quad\cdots \qquad\qquad\quad \cdots \\
&+(n-1) : \text{left side of } \mathcal{C}_1^L
\end{aligned}
$$

Here $\mathcal{C}_k^R$, $\mathcal{C}_k^L$ and $\mathcal{T}_k$ denote the multiple crossing points for the rigth side ($\mathrm{Re}\, q_{n+1} > 0$) and left side ($\mathrm{Re}\, q_{n+1} < 0$) on the real axis, and ordinary turning points of the kth generation, respectively. The range of index is given as $1 \leq m \leq n-1$. We show the ordinary Stokes curves for $n = 3$ with reference points thus introduced in Fig.6.

Since all the solutions are real at the position '0' we may assume the form of the

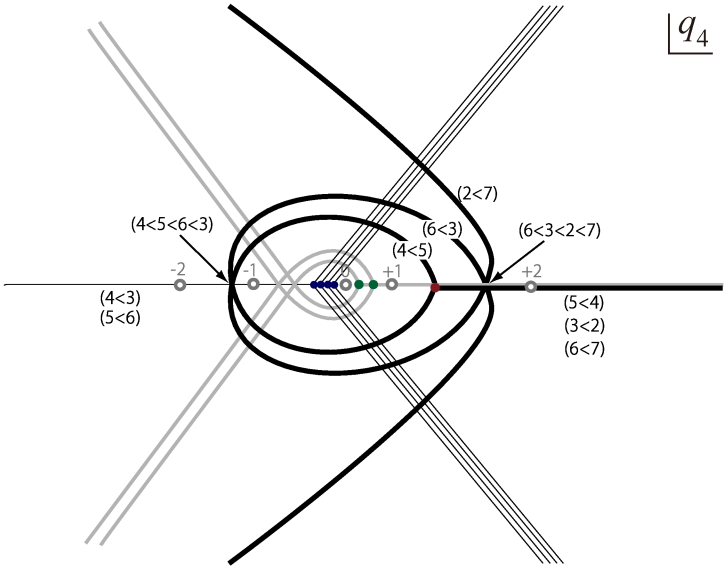

Figure 6. Ordinary turning points and ordinary Stokes curves for the $n = 3$ case (schematic). The bold, gray and thin curves represent the Stokes curves for the 1st, 2nd and 3rd generation, respectively. The number of reference points defined in the text are attached on the real axis.

solution at '0' is expressed as

$$0: \quad u_1 + c_2 u_2 + \cdots + c_{2^n} u_{2^n}, \tag{4.1}$$

without loss generality. Here $c_2, \cdots, c_{2^n}$ are some constants which will be determined by taking into account the boundary conditions. We start from the position '0' and proceed both in the rightward and leftward directions, respectively.

Some speculations for the first several steps imply the following recursion procedure to obtain the contributing solutions consistent with the boundary conditions:

1. for the position '0', assume the linear combination of 2^n solutions given as (4.1).
2. for the position '$+m$', decompose 2^n solutions into 2^{n-m-1} blocks, each of which is composed of 2^{m+1} solutions, and apply the rule established in the connection from '$+(m-1)$' to '$+m$' in the case of the $(m+1)$-step to each block.
3. for the position '$-m$', decompose 2^n solutions into 2^{n-m-1} blocks, each of which is composed of 2^{m+1} solutions, and apply the rule established in the connection from '$-(m-1)$' to '$-m$' in the case of the $(m+1)$-step to each block.
4. repeat these steps for $1 \leq m \leq n-2$.
5. for the position '$\pm m$', perform the connection through the rightmost (resp. leftmost) multiple crossing point.

Our problem is then reduced to finding a systematic algorithm for the last step (v). Using the diagram introduced in subsection 4.1, we can derive a generic procedure for the last step connection (v) especially for the $\mathrm{Re}\, q_{n+1} < 0$ direction. That for the $\mathrm{Re}\, q_{n+1} > 0$ direction is almost the same.

To be concrete we explain it for the $n = 5$ case. Our assumption is that the combination of the solutions at '$+3$' is already known, thus we may assume the combination at '$+4$' is expressed with some constant α as

$$\begin{aligned} +4 : (&\boxed{1}\ 2\ \boxed{3}\ 4\ \boxed{5}\ 6\ 7\ 8\ \boxed{9}\ 10\ 11\ 12\ 13\ \boxed{14}\ 15\ \boxed{16}) \\ &+\alpha(\boxed{17}\ 18\ \boxed{19}\ 20\ 21\ 22\ 23\ \boxed{24}\ 25\ 26\ 27\ \boxed{28}\ 29\ \boxed{30}\ 31\ \boxed{32}). \end{aligned}$$

Here boxed numbers represent the solutions remaining in each position, and non-boxed ones those solutions which have to be removed due to the boundary conditions. Note that the pattern of contributing solutions is symmetric with respect to the center, Except for the solutions u_{16} and u_{17}, all other solutions are recessive in the $\mathrm{Re}\, q_{n+1} > 0$ direction (u_1 and u_{32} are neutral since they are real solutions), and so an unknown constant α can be determined by the boundary condition for u_{16} and u_{17}. Here u_{16} is dominant in the $\mathrm{Re}\, q_{n+1} > 0$ direction, and thereby should be dropped. This fixes our unknown constant α uniquely.

We do not pursue which solutions should be automatically removed from the contribution in the $\mathrm{Re}\, q_{n+1} > 0$ direction. Instead we turn our attention on the $\mathrm{Re}\, q_{n+1} < 0$ side. Using the combination of solutions at '-3' for $n = 4$ (see above), we may express the combination at '-4' as

$$\begin{aligned} -4 : (&\boxed{1}\ 2\ 3\ 4\ 5\ 6\ 7\ 8\ \boxed{9}\ 10\ 11\ 12\ 13\ 14\ 15\ \boxed{16}) \\ &+\alpha(\boxed{17}\ 18\ 19\ 20\ 21\ 22\ 23\ \boxed{24}\ 25\ 26\ 27\ 28\ 29\ 30\ 31\ \boxed{32}) \end{aligned}$$

Note that the last step connection has not yet been taken into account in the above pattern.

From the general formula (3.10) for the number of multiple crossing points in the negative direction we have $N_5^{neg} = 5$, and the corresponding diagram like Fig.5 tells us which solutions are involved in the last step ('-3' $\to$ '-4') connection.

Considering that the remaining pairs that might cause connections from '-3' $\to$ '-4' are $u_9 \leftrightarrow u_{24}$C $u_{16} \leftrightarrow u_{17}$, and the dominance relations for the associated multiple crossings are expressed as $(24 < 9 < 10 < 23)$ and $(16 < 17 < 18 < 15)$, we finally obtain the combination at '-4' as

$$\begin{aligned} -4 : (&\boxed{1}\ 2\ 3\ 4\ 5\ 6\ 7\ 8\ \boxed{9}\ 10\ 11\ 12\ 13\ 14\ 15\ 16) \\ &-i(\boxed{17}\ 18\ 19\ 20\ 21\ 22\ 23\ 24\ 25\ 26\ 27\ 28\ 29\ 30\ 31\ \boxed{32}). \end{aligned}$$

Notice that the mechanism of non-trivial cancellation of decaying solutions u_{16} and u_{24} is the same as remarked in the previous steps. There finally remain 4 solutions in the negative real direction.

We generalize the above procedure for generic n cases. Let P_n be the number of remaining solutions in the $\mathrm{Re}\, q_{n+1} < 0$ direction at the step n. We here derive a recursion relation for P_n. For the sake of convenience we also introduce Q_n which specifies the number of solutions which remain as the contributing solutions at the step n, but are not involved in the connections at multiple crossing points in the negative real axis at the step n. For example, in the $n = 5$ case, $P_n = 4$ as shown above, and $Q_{n-1} = 1$. The solution for the latter is u_1, which is not involved in any connection in the negative real axis.

Let M_n be the number of leftmost solutions in the range $P_{n-1} - Q_n$, then we have

$$M_n = 2^{n-1} - 1 - 2\Big(\Big[\frac{N_n + 1}{2}\Big] - 1\Big). \tag{4.2}$$

Here N_n stands for the number of intersection points of multiple crossing points, which was given as (3.9). From the following inequality,

$$2^{n-3} + 1 < M_n < 2^{n-2} - 2^{n-5}, \tag{4.3}$$

which can be easily proved, we know that the solution u_{M_n} is located between $u_{2^{n-3}+1}$ and $u_{2^{n-2}-2^{n-5}}$. Hence the partner of the solution $u_{2^{n-2}-2^{n-5}}$ is to be cancelled and the solution $u_{2^{n-3}+1}$ and its partner remain. The cancellation occurs under the same mechanism as described above. We then reach a coupled recursion relation for P_n and Q_n as

$$\begin{cases} P_n = 2Q_n + (P_{n-1} - Q_{n-1}), \\ Q_n = P_{n-3}, \end{cases} \tag{4.4}$$

which is reduced to the recursion relation for P_n:

$$P_{n+3} - P_{n+2} - P_n = 0 \qquad (n \geq 2). \tag{4.5}$$

The general solution of this recursion relation is easily obtained as

$$\begin{aligned} P_n = {} & \frac{\alpha^{n-1}(P_3 - (\beta+\gamma)P_2 + \beta\gamma P_1)}{(\alpha-\beta)(\alpha-\gamma)} + \frac{\beta^{n-1}(P_3 - (\gamma+\alpha)P_2 + \gamma\alpha P_1)}{(\beta-\gamma)(\beta-\alpha)} \\ & + \frac{\gamma^{n-1}(P_3 - (\alpha+\beta)P_2 + \alpha\beta P_1)}{(\gamma-\alpha)(\gamma-\beta)} \end{aligned}$$

where α, β and γ are solutions of the characteristic equation for the recursion relation (4.5)

$$x^3 - x^2 - 1 = 0,$$

and are given respectively as

$$\alpha = \frac{1}{3} + \frac{1}{3}\sqrt[3]{\frac{29}{2} - \frac{3\sqrt{93}}{2}} + \frac{1}{3}\sqrt[3]{\frac{1}{2}\left(29 + 3\sqrt{93}\right)} = 1.465571232\cdots .$$

$$\beta = \frac{1}{3} - \frac{1}{6}\left(1 + i\sqrt{3}\right)\sqrt[3]{\frac{29}{2} - \frac{3\sqrt{93}}{2}} - \frac{1}{6}\left(1 - i\sqrt{3}\right)\sqrt[3]{\frac{1}{2}\left(29 + 3\sqrt{93}\right)},$$

$$\gamma = \frac{1}{3} - \frac{1}{6}\left(1 - i\sqrt{3}\right)\sqrt[3]{\frac{29}{2} - \frac{3\sqrt{93}}{2}} - \frac{1}{6}\left(1 + i\sqrt{3}\right)\sqrt[3]{\frac{1}{2}\left(29 + 3\sqrt{93}\right)}.$$

We already know the initial terms as

$$P_2 = 1, \quad P_3 = 2, \quad P_4 = 3.$$

Since $|\beta| = |\gamma| = 0.8260313577\cdots$, P_n grows as

$$P_n \sim \alpha^{n-1} \qquad (n \to \infty).$$

It should be noted that, due to the cancellation between solutions, the growth rate of remaining solutions is not $\log 2$, the topological entropy of the horseshoe dynamics, but non-trivial entropy $\log \alpha = \log\left(1.465571232\cdots\right)$ appears.

In conclusion, our analysis reveals that the birth and death of the WKB solutions caused by the Stokes phenomenon do not occur in a local but entirely global manner, reflecting topological nature encoded in the Stokes geometry. We have derived an explicit general formula to enumerate the number of WKB solutions in the asymptotic region and obtain its growth rate, which is shown to be less than the topological entropy of the corresponding classical dynamics.

References

[1] Friedland S and Milnor J 1989 Dynamical properties of plane polynomial automorphisms *Ergod. Th. Dyn. Sys.* **9** 67–99

[2] Berry M V, Nye J F and Wright F J 1979 The elliptic umbilic diffraction catastrophe *Phil. Trans. R. Soc.* A 291, 453–84

[3] Berry M V and Upstill C 1980 Catastrophe Optics: Morphologies of Caustics and Their Diffraction Patterns *Prog. Opt.* **18** 257–346

[4] Devaney R and Nitecki Z 1979 Shift automorphisms in the Hénon mapping *Commun. Math. Phys.* **67** 137–46

[5] Sterling D, Dullin H R and Meiss J D 1999 Homoclinic bifurcations for the Hénon map *Physica* D **134** 153–84

[6] Cvitanović P, Gunaratne G and Procaccia I 1988 Topological and metric properties of Hénon type strange attractors Phys.Rev. A **38** 1503–20

[7] Cvitanović P 1991 Periodic orbits as the skeleton of classical and quantum chaos *Physica* D **51** 138–51
[8] Shudo A and Ikeda K S 2008 Stokes geometry for the quantum Hénon map *Nonlinearity* **21** 1831–80
[9] Berk H L, Nevins W M and Roberts K V 1982 New Stokesf line in WKB theory *J. Math. Phys.* **23** 988–1002
[10] Aoki T, Kawai T and Takei Y 1994 New turning points in the exact WKB analysis for higher-order ordinary differential equations in *Méthodes résurgentes, Analyse algébrique des perturbations singuliéres*, L. Boutet de Monvel ed. pp. 69–84
[11] Pham F 1967 *Introduction a l'étude topologique des singularités de Landau*, **164** (Mémorial des Sciences Mathématiques)
[12] Berry M V and Howls C J 1991 Hyperasymptotics for integrals with saddles *Proc. L. Soc. London* A **434** 657–75
[13] Howls C J 1997 Hyperasymptotics for multidimensional integrals, exact remainder terms and the global connection problem *Proc. R. Soc. London* A **453** 2271–94
[14] Olde Daalhuis A.B 1998 Hyperasymptotic solutions of higher order linear differential equations with a singularity of rank one *R. Soc. Lond. Proc. Ser. A Math. Phys. Eng. Sci.* **454** 1 – 29.
[15] Delabaere E and Howls C J 2002 *Global asymptotics for multiple integrals with boundaries* Duke Math. J. **112** 199-264.
[16] Kaminski D 1994 Exponentially improved stationary phase approximations for double integrals *Methods Appl. Analysis* **1** 44–56
[17] Fedoryuk M V 1977 *The saddle-point method* Metod perevala (Moskow, Nauka).
[18] Aoki T, Kawai T, Koike T, Sasaki S, Shudo A and Takei Y 2005 A background story and some know-how of virtual turning points *RIMS Kokyuroku* **1424** 53-63
[19] Aoki T, Honda N, Kawai T, Koike T, Sasaki S, Shudo A and Takei Y 2007 Virtual turning points — A gift of microlocal analysis to the exact WKB analysis "*Algebraic Analysis of Differential Equations — from Microlocal Analysis to Exponential Asymptotics — Festschrift in Honor of Takahiro Kawai*" (Springer) pp.29-43
[20] Sato M, Kashiwara M and Kawai T 1973 Microfunctions and pseudo-differential equations *Lect. Notes in Math.* **287** 265–529
[21] Morosawa S, Nishimura Y, Taniguchi M and T. Ueda 1999 *Holomorphic dynamics* (Cambridge Univ. Press)